Hyperelasticity Model for Finite Element Analysis of Natural and High Damping Rubbers in Compression and Shear

A. F. M. S. Amin[1]; S. I. Wiraguna[2]; A. R. Bhuiyan[3]; and Y. Okui[4]

Abstract: Rate-independent monotonic behavior of filled natural rubber and high damping rubber is investigated in compression and shear regimes. Monotonic responses obtained from tests conducted in both regimes demonstrate the prominent existence of the Fletcher–Gent effect, indicated by high stiffness at low strain levels. An improved hyperelasticity model for compression and shear regimes is proposed to represent the rate-independent instantaneous and equilibrium responses including the Fletcher–Gent effect. A parameter identification scheme involving simultaneous minimization of least-square residuals of uniaxial compression and simple shear data is delineated. The difficulties of identifying a unique set of hyperelasticity parameters that hold for both compression and shear deformation modes are thus overcome. The proposed hyperelasticity model has been implemented in a general purpose finite element program. Finite element simulations of experiments have shown the adequacy of the proposed hyperelasticity model, estimated parameters, and employed numerical procedures. Finally, numerical experiments were conducted to further explore the potential of the proposed model, and estimated parameters in analyzing rubber layers of a base isolation bearing subjected either to compression or to a combination of compression and shear.

DOI: 10.1061/(ASCE)0733-9399(2006)132:1(54)

CE Database subject headings: Rubber; Base isolation; Material properties; Identification; Compression; Shear; Finite element method; Nonlinear analysis; Damping.

Introduction

Filled natural rubber (NR) is one of the most impressive materials for engineering applications. During the vulcanization process, some particles such as carbon black are added as fillers to improve certain properties of rubber for specific applications. Rubber is widely used in tires, bridge bearings, seals, shock absorbing bushings, tunnel linings, wind shoes, etc. (Treloar 1975; Roeder and Stanton 1983; Ward 1985; Mullins 1987; Castellani et al. 1998). Most of these applications utilize the high deformability and large compressive strength features of rubbers. Recent use of high damping rubber (HDR) in base isolation devices for earthquake resistant structures has added a new dimension to the application of rubbers (Fujita et al. 1990; Carr et al. 1996; Mori et al. 1996; Kelly 1997). Rubber bearings for base isolation devices are usually made with alternating thin horizontal layers of rubbers bonded to steel plates. In the concept of base isolation, the steel plates provide large stiffness under vertical load, while the rubber layers provide low horizontal stiffness, when the structure is subjected to lateral loads (e.g., earthquake, wind, etc.). The devices are usually subjected either to compression or to a combination of compression and shear.

To analyze rubber bearings, different analytical methods (Lim and Herrmann 1987; Herrmann et al. 1988a,b, 1989; Hwang and Ku 1997; Kelly 1997) that view rubber bearings as an equivalent homogeneous orthotropic continuum are available. Recently, Chang (2002) proposed another formulation: an analytic stiffness matrix to model laminated rubber bearings. These methods, however, cannot discretely model the behaviors of the rubber and steel, and therefore have substantial limitations in predicting local stress and strain conditions within the rubber layers. Furthermore, in practical applications, bearings are often made with tapered cross sections (AASHTO 1992; Ramberger 2002) so as to accommodate inclined girders on the top of a horizontal abutment. In other cases, V-shaped steel plates are used (European Commission 1999) instead of horizontal ones. However, no analytical method is hitherto available to analyze bearings having these various configurations. In this situation, to analyze rubber bearings by resolving the stress fields in rubber layers, at present two paths can be followed: physical testing of the prototypes or numerical analysis on computers using a finite element (FE) technique. While both methods have their own difficulties, from a design and performance evaluation point of view, numerical analysis is more suitable and versatile. Nevertheless, the core of a reliable FE analysis of rubber bearings at the outset relies on a constitutive model that provides adequate representation of the material behavior (Nicholson et al. 1998) both in compression and shear deformations. These constitutive models are described following large deformation theories that take geometric and material non-

[1]Associate Professor, Dept. of Civil Engineering, Bangladesh Univ. of Engineering and Technology, Dhaka 1000, Bangladesh. E-mail: samin@ce.buet.ac.bd

[2]PT. Jasa Marga (Persero), Indonesia Highway Corporation, Padalarang Bypass Project, Plaza Tol TMII, Jakarta 13550, Indonesia.

[3]Dept. of Civil Engineering, Chittagong Univ. of Engineering and Technology, Chittagong 4349, Bangladesh.

[4]Associate Professor, Dept. of Civil and Environmental Engineering, Saitama Univ., 255 Shimo Okubo, Saitama 338-8570, Japan (corresponding author). E-mail: okui@post.saitama-u.ac.jp

Note. Associate Editor: Francisco Armero. Discussion open until June 1, 2006. Separate discussions must be submitted for individual papers. To extend the closing date by one month, a written request must be filed with the ASCE Managing Editor. The manuscript for this paper was submitted for review and possible publication on July 13, 2004; approved on March 22, 2005. This paper is part of the ***Journal of Engineering Mechanics***, Vol. 132, No. 1, January 1, 2006. ©ASCE, ISSN 0733-9399/2006/1-54–64/$25.00.

linearities into account. Moreover, constitutive parameters for such models must have the capability to depict the material responses in these two deformation modes.

The monotonic behavior of rubbers is dominated by a nonlinear rate-dependent elastic response (Aklonis et al. 1972). Under cyclic loading however, rubbers display other inelastic effects, e.g., hysteresis (Gent 1962a,b), Mullins' softening effect (Mullins 1969), and residual strain (Bueche 1960). All these effects are more prominent in HDR. Hence, to model and analyze NR and HDR using a FE procedure, the general constitutive model should be capable of representing these effects. Yet, rubbers are usually modeled using hyperelasticity models (Charlton et al. 1994; Nicholson et al. 1998) to determine the stress distribution under monotonic loading. Such models are expressed in terms of a strain energy density function, W. In the derivation of the functions, deformation is assumed to completely recover to the initial state. Besides, W is assumed to depend only on the final state of strain and be independent of the loading history. Such a model essentially represents a rate-independent response and works as a major component for a more general model representing other inelastic effects as well (Bonet and Wood 1997). Therefore, as an elementary step, this current work considers modeling the rate-independent monotonic behavior under compression and shear through a hyperelasticity model, and its implementation in a FE code.

In this context, earlier work by Jankovich et al. (1981), Häggblad and Sundberg (1983), Mattheck and Erb (1991), and Peng and Chang (1997) in developing FE procedures for analyzing NR parts under tension is noted. Ali and Abdel-Ghaffar (1995) also presented a FE procedure for analyzing the rubber layers of a NR bearing under axial compression. Results from the FE analysis of NR bearings under axial compression, and comparison with analytic solutions, were also reported by Imbimbo and Luca (1998). There, the analytical solution was conformed to FE results for bearings with thinner rubber layers. For bearings with thicker layers of rubber, however, poor agreement was noted, indicating the significance in constitutive modeling. In a contemporary work (Hamez et al. 1998), stress states in a rubber bearing subjected to compression and shear were investigated theoretically using some assumed values of constitutive parameters. In this numerical work the authors tried different hyperelasticity models as described in different literature. Yet, there are limitations in the present state-of-the-art in providing an adequate hyperelasticity model and valid model parameters that can be utilized for analyzing NR and HDR subjected to compression and shear. Thus, scientific interest in these published works using the FE approach is restricted only to the theoretical stress analysis of rubber layers rather than providing the tools for a practical challenge that a designer may encounter in analyzing a NR or HDR bearing. This current work aims to resolve this issue from a realistic viewpoint, and to develop a general procedure for practical application.

Present State-of-the-Art

Rubbers fall into the class of highly deformable solids exhibiting large deformation under a comparatively small load. When a solid body is subjected to a large deformation, the relationship of positions in deformed and undeformed configurations is described by a deformation gradient tensor $\mathbf{F}$

$$\mathbf{F} = \sum_{\alpha=1}^{3} \lambda_\alpha \mathbf{n}_\alpha \otimes \mathbf{N}_\alpha := \begin{bmatrix} F_{11} & F_{12} & F_{13} \\ F_{21} & F_{22} & F_{23} \\ F_{31} & F_{32} & F_{33} \end{bmatrix} \tag{1}$$

where λ_1, λ_2, and λ_3=stretches in the three principal directions; and $\lambda = 1 + dL/L$, with L being the undeformed length. $\mathbf{N}_1, \mathbf{N}_2, \mathbf{N}_3$, and $\mathbf{n}_1, \mathbf{n}_2, \mathbf{n}_3$=material vector triads and spatial vector triads, respectively. The left Cauchy Green deformation tensor, $\mathbf{B}$, describes the strain, while the Cauchy stress tensor, $\mathbf{T}$, describes the stress

$$\mathbf{B} = \mathbf{F}\mathbf{F}^T = \sum_{\alpha=1}^{3} \lambda_\alpha^2 \mathbf{n}_\alpha \otimes \mathbf{n}_\alpha \tag{2}$$

$$\mathbf{T} = -p\mathbf{1} + 2\frac{\partial W}{\partial I_1}\mathbf{B} - 2\frac{\partial W}{\partial I_2}\mathbf{B}^{-1} \tag{3}$$

where

$$I_1 = \text{tr}\,\mathbf{B}$$

$$I_2 = \tfrac{1}{2}\{(\text{tr}\,\mathbf{B})^2 - \text{tr}(\mathbf{B}\mathbf{B})\}$$

$$I_3 = \det \mathbf{B} \tag{4}$$

where I_1, I_2, and I_3=strain invariants. The hydrostatic pressure p is constitutively indeterminate, and hence it is obtained from the underlying equilibrium and boundary conditions of the particular problem. Based on the isotropic assumption, the strain energy density function W is expressed as a function of the strain invariants (Rivlin 1948a,b):

$$W = W(I_1, I_2, I_3) \tag{5}$$

Since rubbers are considered to fall in the class of incompressible materials exhibiting very small volumetric deformation compared to the distortional deformation, the value of I_3 is usually assumed to be unity. Thus, in a strain-invariant based incompressible hyperelasticity model, the description of W as a function of I_1 and I_2 forms the basis of the approach. Alternatively, on the basis of the Valanis and Landel hypothesis (Valanis and Landel 1967), W can also be expressed directly as a function of the three principal stretches, namely, λ_1, λ_2, and λ_3. A rigorous mathematical interpretation is available (Treloar 1975) to show that both approaches are equivalent.

Due to strong dependence of the stress response on the state of strain, experiments are required to identify an adequate form of W. Ideally, such a function should have the capability to predict responses for all possible deformation modes. Among the strain-invariant-based models, the Mooney–Rivlin model (Mooney 1940; Rivlin 1948a,b) is the oldest one. Yet, simpler forms of the Mooney–Rivlin model had limitations in representing the hardening feature that exists at large strain levels. Tschoegl (1972) investigated the use of different higher order terms of the Mooney–Rivlin relation for better reproduction. Subsequently, other versions of hyperelasticity models appeared (Hart-Smith 1966; Alexander 1968; Yamashita and Kawabata 1992; Arruda and Boyce 1993) that better represented the hardening feature at large strains. Yeoh (1990) noted the limitations of Mooney–Rivlin in representing simple shear deformation. A cubic function for the strain energy density that is applicable for both tension and simple shear regimes was also proposed. Recently, Yoshida et al. (2004a,b) used the Yamashita–Kawabata model to represent the elastic behavior of NR and HDR in an elastoplastic model that

reproduces the large strain cyclic responses in uniaxial tension and simple shear regimes. In addition to the strain-invariant-based models, principal stretch-based models (Ogden 1972; Peng and Landel 1972) were also found to adequately predict the large strain uniaxial tension responses.

Most of the published work is aimed at predicting NR responses in a large tension regime. Until recently only a few of these reported the behavior of NR in compression and shear regimes, whereas no thorough work has been undertaken on the behavior of HDR. Furthermore, while all the attention was being paid to representing large strain monotonic responses of rubbers through different hyperelasticity models, there have been reports of difficulties with these models in representing the responses at small strain levels (Yeoh 1990, 1993, 1997) distinguished by high stiffness (modulus). This feature has been referred to recently as the Fletcher–Gent effect (Ahmadi et al. 2003) after the work of Fletcher and Gent (1953) who first discussed the role of fillers on the appearance of the phenomena in filled NR under simple shear. The phenomenon was also observed by Payne and Whittaker (1971) on NR and more recently by Dorfmann and Burtscher (2000) on HDR in different deformation modes, including compression and simple shear. The practical necessity of modeling the Fletcher–Gent effect is quite obvious (Davis et al. 1994), when we consider that base isolation bearings are subjected to low amplitude movement due to service traffic loads, as an example (Chen and Ahmadi 1992). Recently, Amin et al. (2002) revisited the Fletcher–Gent effect while studying the monotonic behavior of NR and HDR in compression. There, the feature was found to have direct dependence on the applied strain rate. Due to the presence of a higher proportion (31%) of filler (Kelly 1997), HDR exhibits the effect much more prominently than NR. Yet, the clear limitations of the conventional hyperelasticity models in representing the phenomenon in small compression strains for both NR and HDR is revealed from the investigation (Amin et al. 2002). To this end, an improved hyperelasticity model was proposed for the compression regime and the enhanced capability achievable with the new model was verified. However, any model that can represent both compression and shear responses of NR and HDR is yet to appear. This suggests the need for further study of the behavior of NR and HDR under compression as well as shear with a view to developing an adequate hyperelasticity model applicable to these two deformation modes.

In modeling the behavior of rubbers subjected to several deformation modes, a certain amount of ambiguity arises in identifying the parameters of a hyperelasticity model. The parameters are generally estimated by using a curve-fitting technique. Hence, they are solely based on their fit to experimental data (James et al. 1975a,b; Treloar 1975; Quigley et al. 1995). Over the years, different researchers have noted that the constitutive parameters of a hyperelasticity model determined from tests at a particular deformation mode are not valid for other modes. To solve this problem, earlier work examined the parameters identified from uniaxial tension, planar tension (pure shear), and biaxial tension deformations. These deformations are solely involved in the diagonal elements (F_{11}, F_{22}, and F_{33}) of the deformation gradient tensor [**F**, Eq. (1)]. Charlton et al. (1994) mention that the parameters determined from uniaxial test data fail in predicting biaxial or planar tension (pure shear) responses. Similar notions are also well documented in other published works (Quigley et al. 1995; Anand 1996; Boyce and Arruda 2000; Seibert and Schöche 2000). To resolve the problem, Gendy and Saleeb (2000) proposed a nonlinear material parameter estimation scheme. The scheme used a differential form of the Ogden hyperelasticity model along with a sensitivity analysis and an optimization procedure to obtain the parameters. The set of parameters determined with this approach by using uniaxial tension, biaxial tension, and planar tension (pure shear) data from Treloar (1944) were found to perform well in these deformation modes.

Yet, the problems associated with identifying parameters for unaxial compression–tension and simple shear deformation involving diagonal and nondiagonal elements of the **F** tensor remained unsolved. In contrast to the uniaxial, biaxial and planar tension (pure shear) deformations that are related to the diagonal elements (F_{11}, F_{22}, and F_{33}) of **F** tensor, a nondiagonal element (F_{12}) is relevant to simple shear deformation. Yeoh (1993) made an early report of work on this problem, when the hyperelasticity parameters of his model determined from simple shear experiments were found to be inadequate for uniaxial tension–compression responses on the same material. Later, Yeoh (1997) examined the Ogden model (1972) and the available curve-fitting algorithms of different commercially available FE software (*ABAQUS* 1996 and *MARC* 1996) in predicting simple shear response. In these programs, uniaxial test data were used to fit the Ogden model and estimate the parameters. Yeoh observed gross overestimation in the prediction of simple shear response using these parameters. In this same context, Gendy and Saleeb (2000) performed a verification trial for estimating parameters from compression and simple shear data using the nonlinear parameter estimation scheme proposed in their paper. The performance of their approach was compared with another one available in commercially available FE software (*ABAQUS* 1996). However, in both cases, the evaluations of the performance were found not to give enough confidence for large strain simple shear response. Furthermore, van den Bogert and de Borst (1994) explicitly showed the limitations of the hyperelasticity parameters determined from a uniaxial tension experiment in predicting the responses of rubber subjected simultaneously to compression and shear. At this time there is no method that can identify a unique set of hyperelasticity parameters for compression and simple shear deformation. This limits wide application of the available general-purpose FE codes for analyzing rubbers that are subjected to compression and shear.

Objectives and Methodology

Our work was aimed first at developing an improved hyperelasticity model that can reproduce the rate-independent monotonic response of NR and HDR under compression and shear. Development of a method to identify a unique set of constitutive parameters from experimental observations carried out in these regimes was addressed next. To make the model applicable for practical application, our work was then directed to implementation of the proposed hyperelasticity model in a general purpose FE code and its verification. The final objective of the work was to explore the potential of the developed FE procedure in analyzing the full-scale laminated NR and HDR bearings that are subjected either to compression or to combinations of compression and shear.

To meet the objectives mentioned above, experiments were carried out on NR and HDR specimens in compression and shear regimes to identify the rate-independent monotonic responses. To this end, the experimental scheme proposed by Amin et al. (2002) was followed to observe the fundamental rate-independent instantaneous and equilibrium responses in the specimens. With a view to working out the generic structure of the hyperelasticity model, the experimental data were considered in detail in regard to the

observed nonlinearities of the stress–strain responses of NR and HDR at different strain levels. A minimization scheme was proposed to estimate unique sets of hyperelasticity parameters for rate-independent monotonic responses of NR and HDR in compression and shear. The proposed hyperelasticity model was incorporated in a general purpose FE code. Three-dimensional (3D) FE simulations of the experiments were performed to verify the adequacy of the proposed hyperelasticity model and parameter identification scheme. Finally, numerical experiments were carried out on rubber blocks having fixed boundary edges and subjected to compression and combinations of compression and shear.

Experiments in Uniaxial Compression and Simple Shear

Specimens of NR and HDR having shear moduli (JIS K 6301) of 0.98 and 0.78 MPa, respectively, were tested under homogeneous compression and simple shear deformations. These rubbers were manufactured at Yokohama Rubber Company, Japan and have application to base isolation bearings. Tests were carried out in a computer-controlled servohydraulic testing machine (Shimadzu Servo Pulser 4800) with a 200 kN load cell. The maximum stroke rate of the load cell crosshead was 50 mm/s. Displacement was applied in the vertical direction on the specimen and the corresponding reaction was obtained from the load cell. Compression specimens were cylindrical in shape measuring 41 mm in height and 49 mm in diameter. A lubricant was used to reduce platen-specimen friction. Thus, it was possible to obtain a homogeneous uniaxial compression deformation. The simple shear specimens ($25\times25\times5$ mm) had a net shear area of 25×25 mm. Dual lap shear specimens (Charlton et al. 1994) were used. Further details of the test setups and procedures are available in Amin (2001), Amin et al. (2002, 2003), and Wiraguna (2003).

Prior to an actual test, each virgin specimen was subjected to a five-cycle preloading at a 0.5/s strain rate to remove the Mullins' softening effect (Mullins 1969). All tests were conducted 20 min after completing the preloading test. Preloaded specimens were tested in compression and shear to identify the fundamental rate-independent responses. By definition, rate-independent equilibrium response is obtained when a rate-dependent material is loaded at an infinitely slow rate, whereas rate-independent instantaneous response is obtained when the material is loaded at an infinitely fast rate. The experimental scheme as proposed by Amin et al. (2002) involving multistep relaxation tests and monotonic tests at different strain rates was followed to identify the responses in compression and simple shear regimes.

Figs. 1 and 2 present these boundary state responses as observed in NR and HDR. Due to the viscosity induced strain-rate effect, the response at the equilibrium state differs significantly from that at the instantaneous state. The effect is visible both in compression and shear deformation modes. The HDR shows the effect more prominently than NR. The stress–strain responses in both states are markedly nonlinear at low, moderate, and large strain levels. The presence of high stiffness at low strain levels, referred to as the Fletcher–Gent effect, is clearly observed in all the stress–strain responses. This feature appeared to be the most prominent in the HDR at its instantaneous state and the weakest in NR at the equilibrium state. In addition, the large deformability at moderate strain levels and a strain-hardening feature at large strain levels were observed. In order to examine the compressibility feature of NR and HDR, volumetric deformation of specimens under uniaxial compression as measured by Amin et al. (2003) were observed. At a stretch of 0.5, NR and HDR were measured as compressed by 2.9 and 1.1% of their respective initial volumes. This indicates the adequacy of assuming the materials to be incompressible. All these observations will be addressed in the next section to introduce a hyperelasticity model to represent the responses.

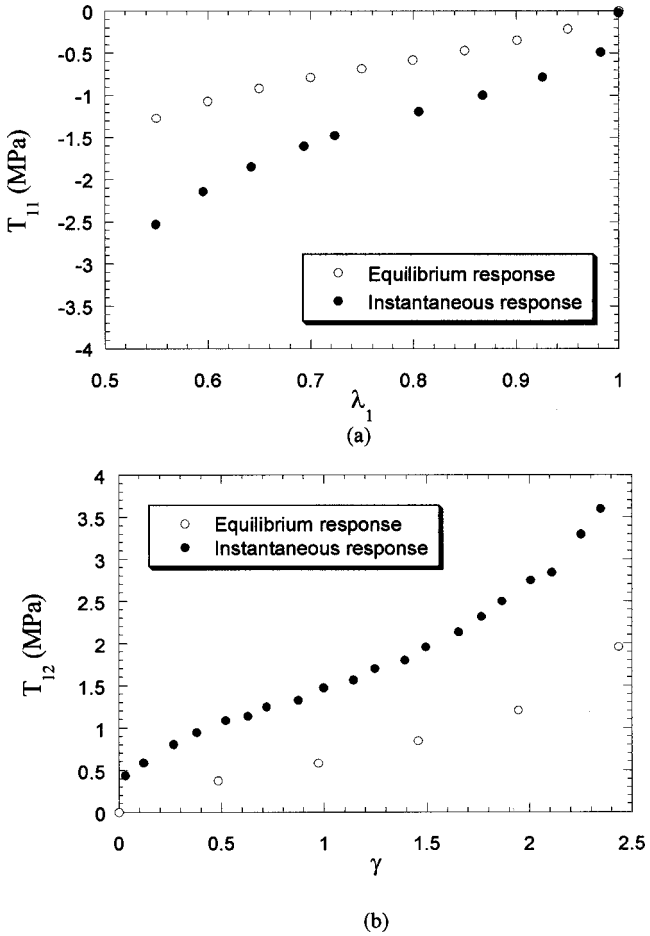

Fig. 1. Monotonic responses obtained from high damping rubber at equilibrium state and instantaneous state: (a) compression and (b) simple shear

Hyperelasticity Model and Parameter Identification

The elementary basis for describing stress–strain response using a hyperelasticity relation has been presented in "Present State-of-the-Art". Further discussion in this section on determining an adequate form of the hyperelasticity relation has clarified the necessity of conducting experiments at relevant deformation modes to consider the strong dependence of stress response on the strain state. In this context, test results are presented in "Experiments in Uniaxial Compression and Simple Shear" to identify the fundamental rate-independent equilibrium and instantaneous responses of NR and HDR obtained in compression and shear regimes. All these will be utilized in this section to propose a hyperelasticity model and a parameter identification scheme. To this end, based on the finite strain theory, the basic descriptions of deformation in these two regimes (Fig. 3) and the associated domains of strain invariants will be considered first.

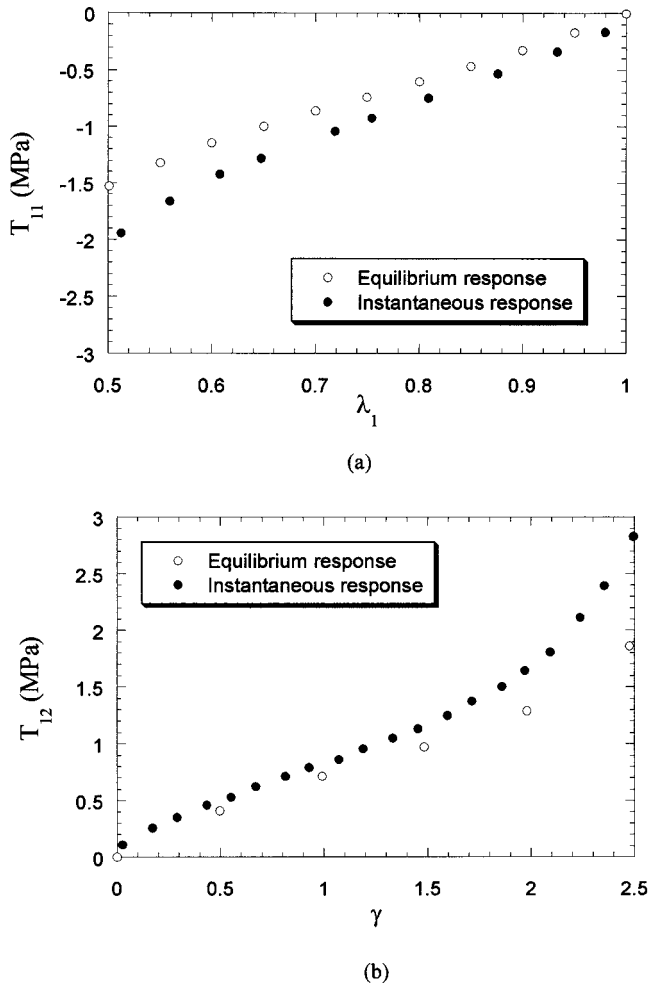

Fig. 2. Monotonic responses obtained from natural rubber at equilibrium state and instantaneous state: (a) compression; and (b) simple shear

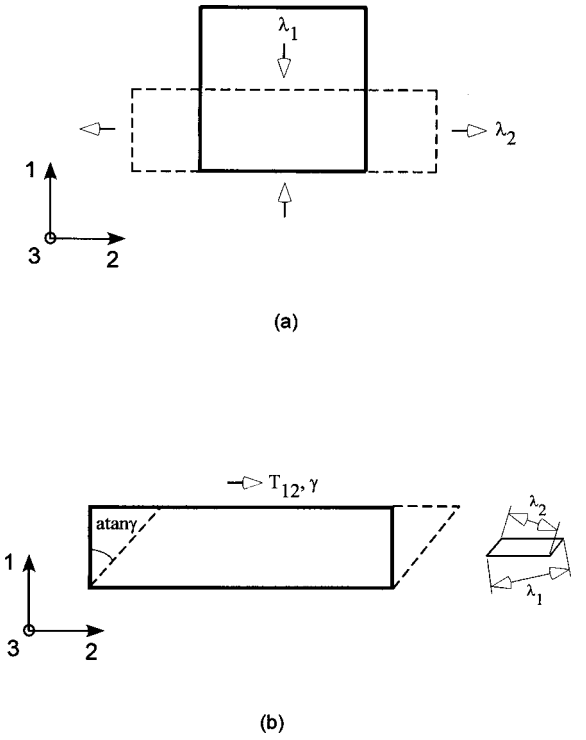

Fig. 3. Fundamental description of deformation: (a) homogeneous uniaxial compression; and (b) simple shear

Uniaxial Compression

When a body is subjected to large homogeneous uniaxial compression, the principal stretch (λ_1) in the loading direction becomes compression [Fig. 3(a)]. Principal stretches in the other two directions (λ_2 and λ_3) become tension. Considering isotropy and incompressibility, we have $\lambda_2^2=\lambda_3^2=\lambda_1^{-1}$. Using Eqs. (1) and (2), the deformation gradient tensor **F** and left Cauchy–Green deformation tensor **B** can be written as

$$\mathbf{F}=\begin{pmatrix}\lambda_1 & 0 & 0\\ 0 & \sqrt{\frac{1}{\lambda_1}} & 0\\ 0 & 0 & \sqrt{\frac{1}{\lambda_1}}\end{pmatrix}\quad \mathbf{B}=\begin{pmatrix}\lambda_1^2 & 0 & 0\\ 0 & \frac{1}{\lambda_1} & 0\\ 0 & 0 & \frac{1}{\lambda_1}\end{pmatrix} \tag{6}$$

Using Eqs. (4) and (5), the strain invariants for uniaxial compression are expressed as

$$I_1=\frac{2}{\lambda_1}+\lambda_1^2\quad I_2=\frac{1}{\lambda_1^2}+2\lambda_1\quad I_3=1 \tag{7}$$

Using Eq. (3), the expression for Cauchy stress T_{11} can be expressed as

$$T_{11}=2\left(\lambda_1^2-\frac{1}{\lambda_1}\right)\left(\frac{\partial W}{\partial I_1}+\frac{1}{\lambda_1}\frac{\partial W}{\partial I_2}\right) \tag{8}$$

Simple Shear

Fig. 3(b) schematically presents the simple shear deformation. In contrast to uniaxial compression, the direction of applied displacement does not coincide with the directions of principal stretches; rather it involves a rotation of axes. Due to applied shear strain (γ), the deformation gradient tensor **F** and the left Cauchy–Green deformation tensor **B** are described as

$$\mathbf{F}=\begin{bmatrix}1 & \gamma & 0\\ 0 & 1 & 0\\ 0 & 0 & 1\end{bmatrix}\quad \mathbf{B}=\begin{bmatrix}1+\gamma^2 & \gamma & 0\\ \gamma & 1 & 0\\ 0 & 0 & 1\end{bmatrix} \tag{9}$$

Using Eqs. (4) and (9), the strain invariants are expressed as

$$I_1=I_2=3+\gamma^2\quad I_3=1 \tag{10}$$

Then the expression for Cauchy stress T_{12} becomes

$$T_{12}=2\gamma\left(\frac{\partial W}{\partial I_1}+\frac{\partial W}{\partial I_2}\right) \tag{11}$$

Using Eq. (2) and taking eigenvalues of the **B** tensor, the principal

stretches, λ_1 and λ_2 associated with shear strain γ can be obtained as

$$\lambda_1 = \sqrt{1 + \frac{\gamma^2}{2} + \gamma\sqrt{1 + \frac{\gamma^2}{4}}} \tag{12}$$

$$\lambda_2 = \sqrt{1 + \frac{\gamma^2}{2} - \gamma\sqrt{1 + \frac{\gamma^2}{4}}} \tag{13}$$

Eq. (12) represents the principal tension stretch, while Eq. (13) represents the principal compression stretch.

Hyperelasticity Model

Representation of incompressible hyperelasticity response depends solely on the definition of $W(I_1, I_2)$. Eqs. (5), (7), (8), (10), and (11) show this fact. Hence, to establish the function W that is applicable for relevant deformation modes, Kawabata et al. (1977, 1981) studied the dependence of $\partial W/\partial I_1$ and $\partial W/\partial I_2$ on I_1 and I_2 using uniaxial and biaxial test data. Their investigation showed that $\partial W/\partial I_1$ and $\partial W/\partial I_2$ depend only on I_1 and I_2, respectively. Based on these findings, W can be split into two individual functions, namely, $f(I_1)$ and $g(I_2)$

$$W(I_1, I_2) = \int f(I_1)dI_1 + \int g(I_2)dI_2 \tag{14}$$

where

$$f(I_1) = \frac{\partial W}{\partial I_1} \quad g(I_2) = \frac{\partial W}{\partial I_2}$$

This idea was further clarified in the work of Lambert-Diani and Rey (1999), where a general procedure for identifying the strain energy density function was proposed. In their work, the effect of the maximum principal stretch λ_1 on the values of I_1 and I_2 in uniaxial tension, planar tension (pure shear), and equibiaxial tension modes were considered. Obviously, all these deformation modes are related to the diagonal components of the **F** tensor, where the applied stretching direction coincides with the directions of principal stretches. Following this approach, Amin et al. (2002) proposed a hyperelasticity model for NR and HDR in a uniaxial compression regime. The model was expressed as a function of I_1 only. Now, in order to include the simple shear response we have revisited the approach of Lambert-Diani and Rey (1999) and compared the effect of maximum principal stretch λ_1 on the values of I_1 and I_2 in uniaxial compression–tension and simple shear modes. To do this, Eqs. (7) and (12) have been used, in Fig. 4, to present the relations between the first and the second strain invariants (I_1 and I_2) with principal stretch λ_1 for uniaxial compression and simple shear deformation. The comparative curves clearly illustrate the effect of I_2 on principal tension stretches ($\lambda_1 > 1$) arising out of simple shear. The necessity to consider the inclusion of $g(I_2)$ in the W function becomes obvious. Following this observation, the original W function as proposed by Amin et al. (2002) is further improved here

$$W(I_1, I_2) = C_5(I_1 - 3) + \frac{C_3}{N+1}(I_1 - 3)^{N+1} + \frac{C_4}{M+1}(I_1 - 3)^{M+1} + C_2(I_2 - 3) \tag{15}$$

where C_5, C_3, C_4, C_2, M, and N=material parameters. Here it should be noted that the explicit form of the newly introduced

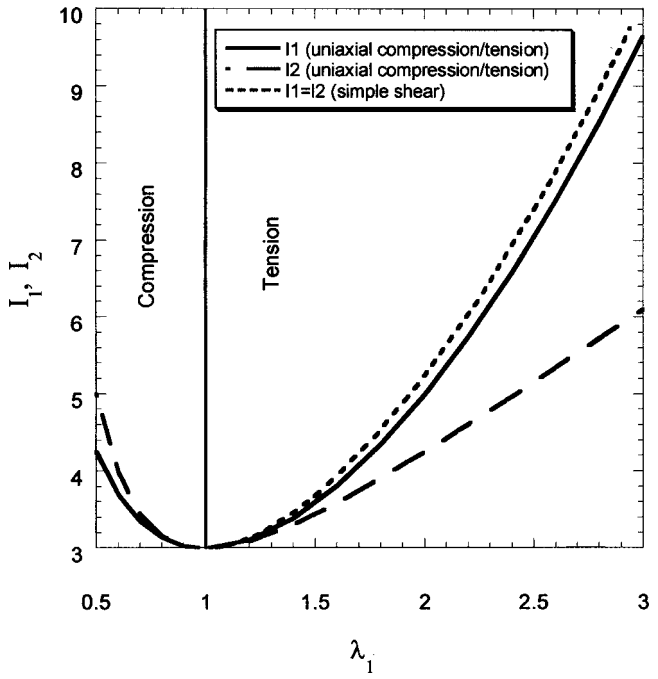

Fig. 4. Domains of first and second strain invariants in uniaxial compression–tension and simple shear deformations

$g(I_2)$ function related to the C_2 parameter is the simplest possible form that exists in the original Mooney–Rivlin model (Mooney 1940; Rivlin 1948a,b). Using Eqs. (8), (11), and (15), the expressions for Cauchy stress in compression and simple shear for the proposed hyperelasticity model can be obtained as

$$T_{11} = 2\left(\lambda_1^2 - \frac{1}{\lambda_1}\right)\left[C_5 + C_3(I_1 - 3)^N + C_4(I_1 - 3)^M + \frac{C_2}{\lambda_1}\right] \tag{16}$$

$$T_{12} = 2\gamma[C_5 + C_2 + C_4\gamma^{2M} + C_3\gamma^{2N}] \tag{17}$$

Here, one can note the case of undeformed state, where $\lambda_1 = 1$, $\gamma = 0$, and $I_1 = I_2 = 3$. Once these values are put in Eqs. (15)–(17), W, T_{11}, and T_{12} become zero. This result agrees with the initial boundary condition that exists in the stress free undeformed state.

Parameter Identification

In order to identify the parameters of the proposed hyperelasticity model, the experimental data obtained in compression and shear regime were used along with a scheme involving the least-square method to minimize the residuals. Fig. 5 presents a schematic of the proposed procedure. To identify parameters for either equilibrium or instantaneous state, initial values of the parameters were assumed to calculate, ξ_i for each compression data point by taking the square of the difference between T_{11} values obtained from experiment and the hyperelasticity relation [Eq. (16)]. Thus, the square of the residuals for each data point was obtained. In a similar fashion, simple shear data was used to calculate η_j for each of the shear data points using Eq. (17). In the following step, summation of the residuals, ξ_i and η_j obtained from compression and shear data was minimized using *Mathematica* (Wolfram 1999). The process is quite simple and straightforward. In such a minimization scheme, the number of data

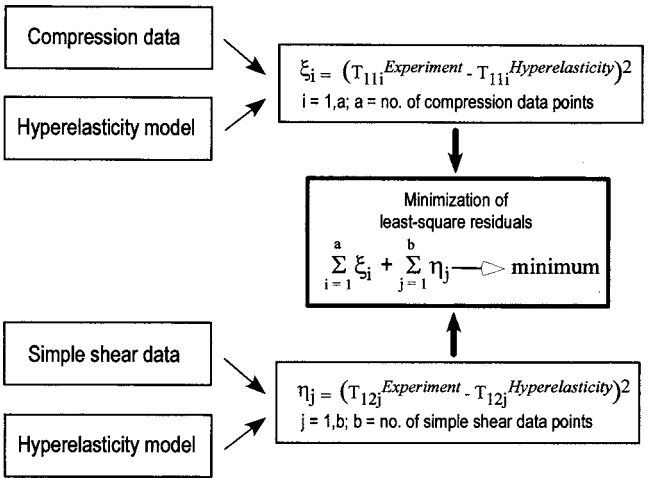

Fig. 5. Parameter identification scheme to identify hyperelasticity parameters by simultaneously using compression and simple shear data

points considered works as a weighting factor. Hence, to give equal weight for compression and shear data, the estimation process considered an equal number of data points ($a=b$) for both the regimes over the strain range. Less than five trials were found to be adequate to obtain a satisfactory fit and to find a unique set of parameters for predicting compression and simple shear responses.

Table 1 presents four sets of the parameters for NR and HDR in the equilibrium state and instantaneous states. Each set of estimated parameters is valid for predicting a relevant response both in compression and shear deformation modes. Figs. 6 and 7 present the experimental data points and the stress–strain responses predicted by the hyperelasticity model and the estimated sets of parameters in compression and shear regimes. The excellent performance of the proposed hyperelasticity model and the parameter identification scheme in representing the experimentally observed responses at low, moderate, and large strain levels is evident.

When the two states are compared, the values (Table 1) of all multiplicative parameters (C_5, C_3, C_4, C_2) at equilibrium state are seen to be consistently smaller than those at instantaneous state for a particular material. However, for exponent type parameters (M and N), each of the materials has constant values in both states. These features help to estimate the parameters for viscosity induced overstress by directly subtracting the instantaneous state values of C_5, C_3, C_4, and C_2 from the equilibrium state values to fit a Maxwell or Kelvin model (Huber and Tsakmakis 2000; Amin et al. 2002). Hence, unconstrained fit was first obtained for the instantaneous state. The multiplicative and exponent type parameters were thus estimated. Subsequently, the values of M and N as finally obtained from instantaneous state trials were introduced as constraints to obtain the fit to estimate the multiplicative

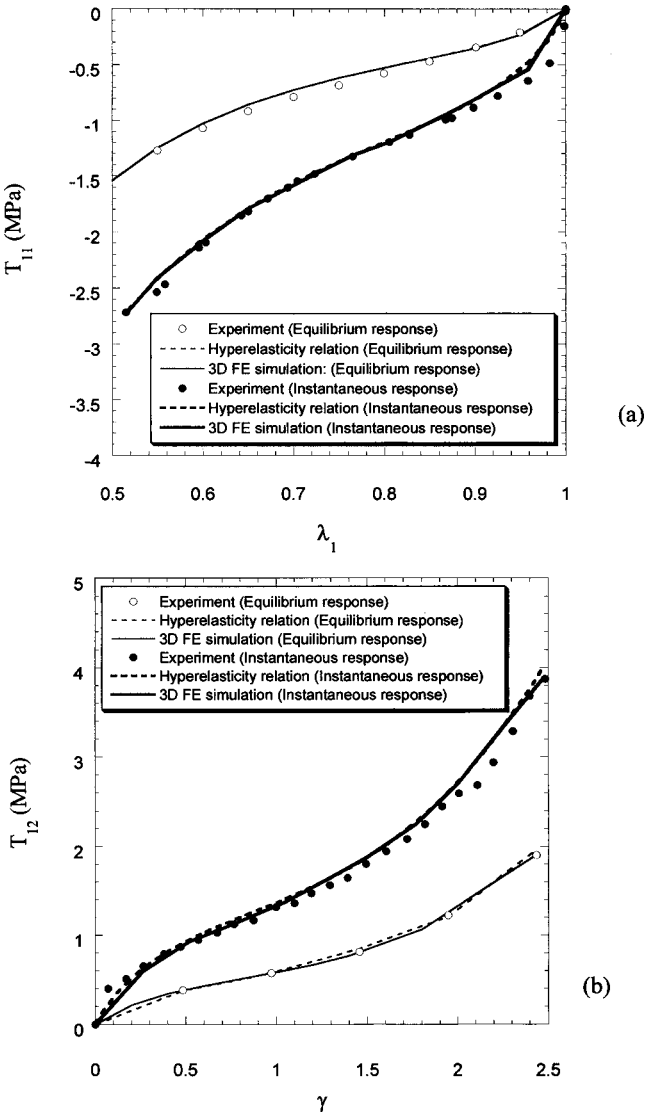

Fig. 6. Representation of rate-independent monotonic responses of high damping rubber using proposed hyperelasticity model and identified parameters. The result obtained from three-dimensional finite element simulation is also presented for comparison: (a) compression and (b) simple shear.

parameters for the equilibrium state. On the other hand, this approach is not required for the case when one evaluates the parameters for simulating monotonic compression and simple shear responses obtained at any other strain rate within the viscosity domain. In such a process, compression and simple shear tests must be conducted at the same strain rate to eliminate the rate-dependency effect from the test data and to obtain some reasonable values of parameters. At this stage, however, we noted a limitation of earlier parameter estimation efforts (Anand 1996;

Table 1. Material Parameters for High Damping Rubber (HDR) and Natural Rubber (NR)

Specimens	Responses	C_2 (MPa)	C_3 (MPa)	C_4 (MPa)	C_5 (MPa)	M	N
HDR	Equilibrium	0.145	1.182	−5.297	4.262	0.06	0.27
	Instantaneous	0.166	2.477	−11.689	9.707		
NR	Equilibrium	0.095	0.019	−0.515	0.754	0.15	1.29
	Instantaneous	0.176	0.043	−0.861	1.056		

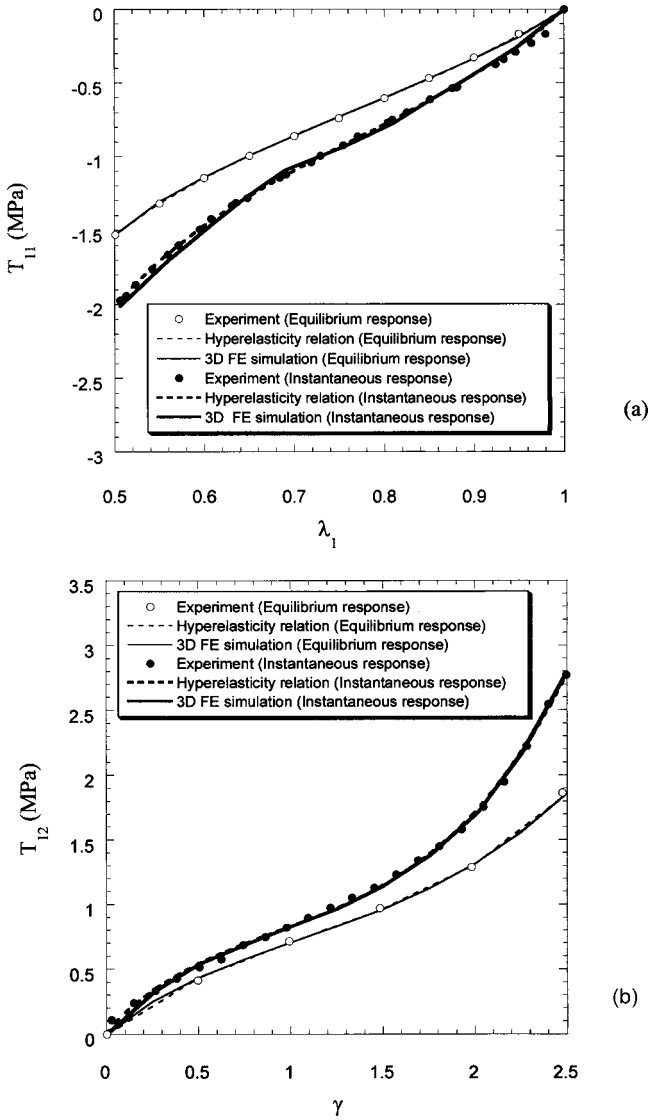

Fig. 7. Representation of rate-independent monotonic responses of natural rubber using proposed hyperelasticity model and identified parameters. Results obtained from three-dimensional finite element simulation are also presented for comparison: (a) compression and (b) simple shear.

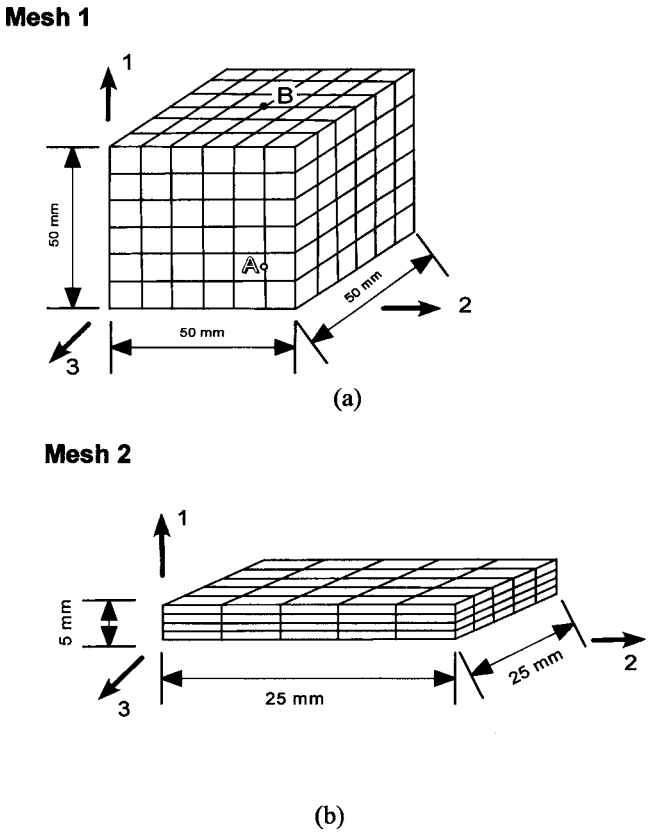

Fig. 8. Finite element mesh used for numerical simulation. (a) Mesh 1. Boundary conditions: Node A at bottom surface (2-3 plane) is restrained in 1, 2, and 3 directions. All other nodes at bottom surface (2-3 plane) are free in 2 and 3 directions and restrained in 1 direction. Node B at top edge is restrained in 2 and 3 directions. All other nodes at top edge are free. Displacement is applied along 1 direction. (b) Mesh 2. Boundary conditions: All nodes at bottom edge (parallel to 2-3 plane) are restrained and fixed in 1, 2, and 3 directions. All nodes at top edge (parallel to 2-3 plane) are restrained in 1 and 3 directions. Displacement is applied along two directions.

Boyce and Arruda 2000; Gendy and Saleeb 2000) for predicting responses in multiple deformation modes using a hyperelasticity model. In all these works, no consideration was given either to using test data for rate-independent responses obtained in the relevant deformation modes or to eliminating the strain-rate effect from the test data employed. This disagrees with the fundamental proposition of hyperelasticity theory that merely depicts a rate-independent response.

Finite Element Implementation and Verification

The proposed hyperelasticity model [Eq. (15)] and the identified parameters (Table 1) were utilized in this section for analyzing rubbers with different loading and boundary conditions. The model was implemented in *FEAP*, a general purpose FE analysis program (Taylor 2000) developed at the Univ. of California at Berkeley, Berkeley, Calif. and partially documented in Zienkiewicz and Taylor (1996). Eight node 3D solid elements formulated on the basis of finite deformation theory were used to model NR and HDR. Figs. 8(a and b) present two different meshes involving 216 (Mesh 1) and 100 (Mesh 2) 3D elements, respectively. To overcome the ill-conditioning problem arising due to incompressible deformation, a penalty function algorithm (Simo and Taylor 1982) was used.

In order to validate the FE implementation process (Bhuiyan 2004), compression and simple shear experiments ("Experiments in Uniaxial Compression and Simple Shear") were simulated using Meshes 1 and 2, respectively. The boundary conditions for both of these two meshes were defined in conformity with the adopted experimental conditions. The instantaneous and equilibrium responses for NR and HDR as obtained from FE simulation are plotted in Figs. 6 and 7. The strong correlation between experiment and simulation for each of the cases over the strain ranges provides confidence for the adopted numerical procedure that fully takes the material nonlinearity into account. Fig. 9 presents the displacement and stress contours for uniaxial compression of HDR response. The homogeneity of deformation (λ_1) pattern [Fig. 9(a)] and stress (T_{11}) distribution [Fig. 9(b)] of the uniaxial compression test can be noted. Fig. 10 presents the stress (T_{12}) contour obtained from simple shear simulation of HDR re-

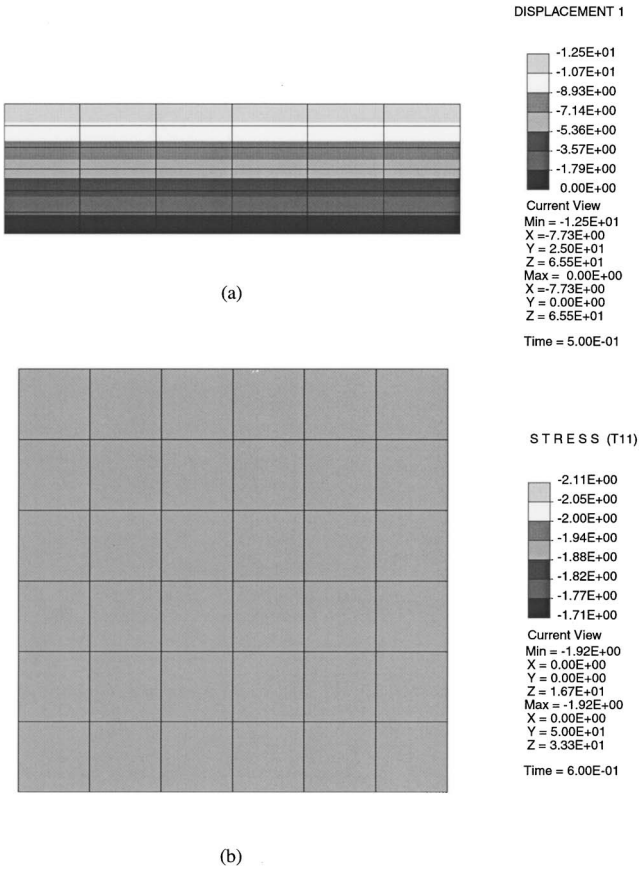

Fig. 9. Numerical simulation of instantaneous response obtained from high damping rubber under uniaxial homogeneous compression experiments using Mesh 1: (a) displacement contours at $\lambda_1=0.70$ and (b) stress contours (T_{11}) at $\lambda_1=0.85$

sponse. In contrast to uniaxial homogeneous compression, some nonuniform distribution of stress is noted here. However, the variation of stress is close enough to be considered uniform.

Finally, in order to examine the potential of using the developed procedure in analyzing rubber bearings, results of some numerical experiments are presented. To do this, the rubbers were modeled using 3D solid elements (Mesh 1), but having a fixed boundary at the edges. The boundaries of the adopted FE mesh thus resemble what exists in a real bearing. The mesh was first

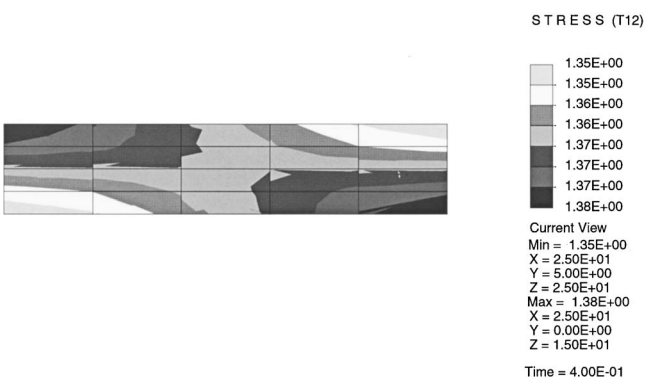

Fig. 10. Numerical simulation of instantaneous response obtained from high damping rubber under simple shear using Mesh 2. Shear stress (T_{12}) contours obtained at $\gamma=1.00$ are shown.

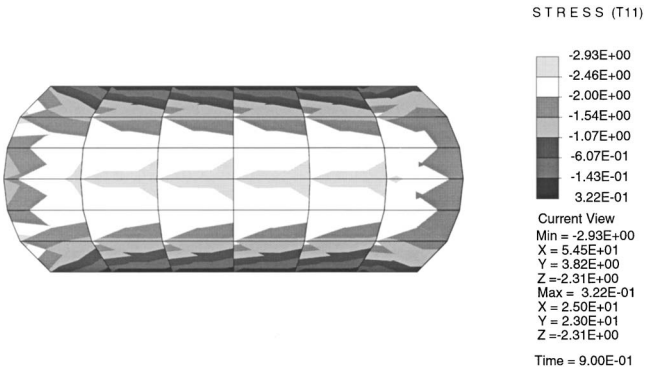

Fig. 11. Numerical experiments on Mesh 1, but with fixed boundary edges and subjected to uniaxial compression. Parameters of high damping rubber at instantaneous state are used with deformed mesh along with T_{11} contour at $\lambda_1=0.70$.

subjected to uniaxial compression. Fig. 11 presents the deformed shape of the mesh delineating deformation along with the stress (T_{11}) contours for HDR. In contrast to Fig. 9, the nonhomogeneity in the distribution of stress arising from the adopted boundary condition can be noted. The simulated stress distribution indicates the existence of a very high compressive stress at the middle of the mesh. Fig. 12 presents the deformed shapes and stress distributions of the mesh subjected to a combination of compression and shear. The deformed mesh indicates the geometric nonlinearities taken into account using the finite deformation formulations. Furthermore, the variation of shear stress (T_{12}) in the block can be noted from the figure. The contours suggest a very high concentration of shear stress in the diagonal direction. In all these FE simulations, incompressible deformation was assumed to simulate responses from small rubber blocks. Yet, in the case of analyzing large base isolation bearings, a plane strain situation exists at the bearing center. In such locations, hydrostatic tension to compression may occur in the bearings resulting in considerable volumetric deformation (Hermann et al. 1988a,b, 1989; Dorfmann and Burtscher 2000). To address this, the proposed hyperelasticity model needed to be modified by incorporating a dilational term involving I_3 [Eq. (5)].

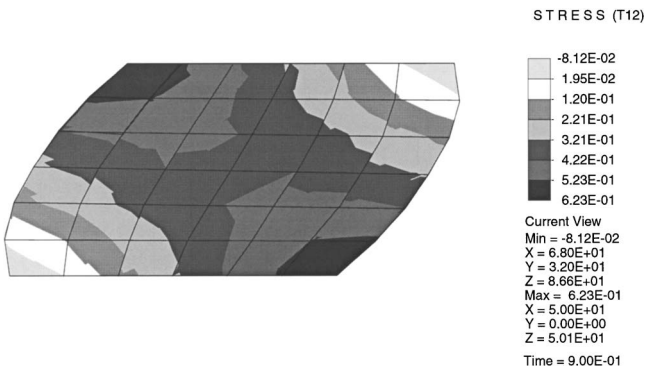

Fig. 12. Numerical experiments on Mesh 1, but with fixed boundary edges and subjected to uniaxial compression and simple shear in combination. Parameters of high damping rubber at instantaneous state are used with deformed mesh along with T_{12} contour at $\lambda_1=0.60$, $\gamma=0.40$.

Conclusions and Further Remarks

1. A typical monotonic response of rubbers is marked by large deformability up to moderate strain levels followed by a strain-hardening feature at large strain levels. However, the responses obtained from NR containing filler and HDR specimens in compression and shear regimes displayed the existence of the Fletcher–Gent effect characterized by high stiffness (modulus) at low strain levels. We took this feature into account and proposed an improved hyperelasticity model to represent the rate-independent elastic responses of NR and HDR in compression and shear.
2. A parameter identification scheme that simultaneously uses the compression and shear data to minimize the least-square residuals is proposed. The scheme was successfully used to identify a single set of parameters applicable for both compression and shear regimes.
3. The proposed hyperelasticity model was implemented in a general-purpose FE code. Numerical simulations of experiments using the proposed model and estimated parameters were conducted for verification purposes. Finally, numerical experiments were carried out on rubber with fixed boundary edges and subjected to different loading combinations. To improve the prediction capability, our work suggests incorporating a volumetric term in the proposed hyperelasticity model to account for the volumetric deformation that may occur in the center locations of a base isolation bearing. The writers expect to address this aspect of the problem in the future.

Acknowledgments

The writers are very grateful to Professor H. Horii, Department of Civil Engineering, University of Tokyo, Japan for his valuable comments and suggestions and particularly for allowing them to use the experimental facilities of his laboratory to carry out the mechanical tests in the investigation. The writers gratefully acknowledge the kind cooperation extended by the Yokohama Rubber Co. by providing test specimens. The writers also sincerely appreciate the funding provided by the Japanese Ministry of Education, Science, Sports, and Culture as a Grant-in-Aid for Scientific Research (C) (Grant No. 12650457) to carry out this research.

References

ABAQUS (1996). *Theory manual, Version 5.6*, Hibbitt, Karlsson & Sorensen, Inc., Providence, R.I.

Ahmadi, H. R., Kingston, J. G. R, Muhr, A. H., Gracia, L. A., and Gómez, B. (2003). "Interpretation of the high–low-strain modulus of filled rubbers as an inelastic effect." *Proc., 3rd European Conf. on Constitutive Models for Rubber*, J. Busfield and A. Muhr, eds., Balkema, Rotterdam, The Netherlands, 357–364.

Aklonis, J. J., Macnight, W. J., and Shen, M. (1972). *Introduction to polymer viscoelasticity*, Wiley, Toronto, Canada.

Alexander, H. (1968). "A constitutive relation for rubber-like materials." *Int. J. Eng. Sci.*, 6, 549–563.

Ali, H. M., and Abdel-Ghaffar, A. M. (1995). "Modeling of rubber and lead passive-control bearings for seismic analysis." *J. Struct. Eng.*, 121(7), 1134–1144.

American Association for State Highway and Transportation Officials (AASHTO). (1992). *Standard specifications for highway bridges*, 15th Ed., Washington, D.C.

Amin, A. F. M. S. (2001). "Constitutive modeling for strain-rate dependency of natural and high damping rubbers." PhD thesis, Saitama Univ., Saitama, Japan.

Amin, A. F. M. S., Alam, M. S., and Okui, Y. (2002). "An improved hyperelasticity relation in modeling viscoelasticity response of natural and high damping rubbers in compression: Experiments, parameter identification, and numerical verification." *Mech. Mater.*, 34, 75–95.

Amin, A. F. M. S., Alam, M. S., and Okui, Y. (2003). "Measurement of lateral deformation of natural and high damping rubbers in large deformation uniaxial tests." *J. Test. Eval.*, 31(6), 524–532.

Anand, L. (1996). "A constitutive model for compressible elastomeric solids." *Comput. Mech.*, 18, 339–355.

Arruda, E. M., and Boyce, M. C. (1993). "A three-dimensional constitutive model for the large stretch behavior of rubber elastic materials." *J. Mech. Phys. Solids*, 41, 389–412.

Bhuiyan, A. R. (2004). "Finite element modeling for nonlinear elastic response of natural and high damping rubber." MSc thesis, Bangladesh Univ. of Engineering and Technology, Bangladesh.

Bonet, J., and Wood, R. D. (1997). *Nonlinear continuum mechanics for finite element analysis*, Cambridge Univ. Press, Cambridge, U.K.

Boyce, M. C., and Arruda, E. M. (2000). "Constitutive models of rubber elasticity: A review." *Rubber Chem. Technol.*, 73, 504–523.

Bueche, F. (1960). "Mechanical degradation of high polymers." *J. Appl. Polym. Sci.*, 4, 101–106.

Carr, A. J., Cooke, N., and Moss, P. J. (1996). "Compression behavior of bridge bearings used for seismic isolation." *Eng. Struct.*, 18, 351–362.

Castellani, A., Kajon, G., Panzeri, P., and Pezzoli, P. (1998). "Elastomeric materials used for vibration isolation of Railaway Lines." *J. Eng. Mech.*, 124(6), 614–621.

Chang, C. (2002). "Modeling of laminated rubber bearings using an analytical stiffness matrix." *Int. J. Solids Struct.*, 39, 6055–6078.

Charlton, D. J., Yang, J., and Teh, K. K. (1994). "A review of methods to characterize rubber elastic behavior for use in finite element analysis." *Rubber Chem. Technol.*, 67, 481–503.

Chen, Y., and Ahmadi, G. (1992). "Wind effects on base-isolated structures." *J. Eng. Mech.*, 118(8), 1708–1727.

Davis, C. K. L., De, D. K., and Thomas, A. G. (1994). "Characterization of the behavior of rubber for engineering design purposes. 1: Stress–strain relations." *Rubber Chem. Technol.*, 67, 716–728.

Dorfmann, A., and Burtscher, S. L. (2000). "Aspects of cavitation damage in seismic bearings." *J. Struct. Eng.*, 126(5), 573–579.

European Commission (1999). "Highly adaptable rubber isolating system (HARIS)." *Final Technical Rep. Contract No. BRPR-CT95-0072*, *Project No. Be-1258*.

Fletcher, W. P., and Gent, A. N. (1953). "Non-linearity in the dynamic properties of vulcanized rubber compounds." *Trans. Inst. Rubber Industry*, 29, 266–280.

Fujita, T., Fujita, S., Tazaki, S., Yoshizawa, T., and Suzuki, S. (1990). "Research, development and implementation of rubber bearings for seismic isolations." *JSME Int. J., Ser. I*, 33, 394–403.

Gendy, A. S., and Saleeb, A. F. (2000). "Nonlinear material parameter estimation for characterizing hyperelastic large strain models." *Comput. Mech.*, 25, 66–77.

Gent, A. N. (1962a). "Relaxation processes in vulcanized rubber. I: Relation among stress relaxation, creep, recovery, and hysteresis." *J. Appl. Polym. Sci.*, 6, 33–441.

Gent, A. N. (1962b). "Relaxation processes in vulcanized rubber. II: Secondary relaxation due to network breakdown." *J. Appl. Polym. Sci.*, 6, 442–448.

Häggblad, B., and Sundberg, J. A. (1983). "Large strain solutions for rubber components." *Comput. Struct.*, 17, 835–843.

Hamzeh, O. N., Tassoulas, J. L., and Becker, E. B. (1998). "Behavior of elastomeric bridge bearings: Computational results." *J. Bridge Eng.*, 3(3), 140–146.

Hart-Smith, L. J. (1966). "Elasticity parameters for finite deformations of rubber-like materials." *Z. Angew. Math. Phys.*, 17, 608–626.

Herrmann, L. R., Hamidi, R., Shafigh-Nobari, F., and Lim, C. K. (1988a). "Nonlinear behavior of elastomeric bearings. I: Theory." *J. Eng. Mech.*, 114(11), 1811–1830.

Herrmann, L. R., Hamidi, R., Shafigh-Nobari, F., and Ramaswamy, A. (1988b). "Nonlinear behavior of elastomeric bearings. II: FE analysis and verification." *J. Eng. Mech.*, 114(11), 1831–1853.

Herrmann, L. R., Ramaswamy, A., and Hamidi, R. (1989). "Analytical parameter study for class of elastomeric bearings." *J. Struct. Eng.*, 115(10), 2415–2434.

Huber, N., and Tsakmakis, C. (2000). "Finite deformation viscoelasticity laws." *Mech. Mater.*, 32, 1–18.

Hwang, J. S., and Ku, S. W. (1997). "Analytical modeling of high damping rubber bearings." *J. Struct. Eng.*, 123(8), 1029–1036.

Imbimbo, M., and Luca, A. D. (1998). "F.E. stress analysis of rubber bearings under axial loads." *Comput. Struct.*, 68, 31–39.

James, A. G., Green, A., and Simpson, G. M. (1975a). "Strain energy functions of rubber. I: Characterization of gum vulcanizates." *J. Appl. Polym. Sci.*, 19, 2033–2058.

James, A. G., and Green, A. (1975b). "Strain energy functions of rubber. II: The characterization of filled vulcanizates." *J. Appl. Polym. Sci.*, 19, 2319–2330.

Jankovich, E., Leblanc, F., and Durand, M. (1981). "A finite element method for the analysis of rubber parts, experimental and analytical assessment." *Comput. Struct.*, 14, 385–391.

Kawabata, S., and Kawai, H. (1977). "Strain energy density functions of rubber vulcanizates from biaxial extension." *Adv. Polym. Sci.*, 24, 90–124.

Kawabata, S., Matsuda, M., Tei, K., and Kawai, H. (1981). "Experimental survey of the strain energy density function of isoprene rubber vulcanizate." *Macromolecules*, 14, 154–162.

Kelly, J. M. (1997). *Earthquake resistant design with rubber*, Springer-Verlag, London.

Lambert-Diani, J., and Rey, C. (1999). "New phenomenological behavior laws for rubbers and thermo plastic elastomers." *Eur. J. Mech. A/Solids*, 18, 1027–1043.

Lim, C. K., and Herrmann, L. R. (1987). "Equivalent homogeneous FE model for elastomeric bearings." *J. Struct. Eng.*, 113(1), 106–125.

MARC (1996). MSC Software Corporation, Redwood City, Calif.

Mattheck, C., and Erb, D. (1991). "Shape optimization of a rubber bearing." *Int. J. Fatigue*, 13, 206–208.

Mooney, M. (1940). "A theory of large elastic deformation." *J. Appl. Phys.*, 11, 582–592.

Mori, A., Carr, A. J., Cooke, N., and Moss, P. J. (1996). "Compression behavior of bridge bearings used for seismic isolation." *Eng. Struct.*, 18, 351–362.

Mullins, L. (1969). "Softening of rubber by deformations." *Rubber Chem. Technol.*, 42, 339–362.

Mullins, L. (1987). "Engineering with rubber." *Chem. Tech. (Leipzig)*, 13, 720–727.

Nicholson, D. W., Nelson, N. W., Lin, B., and Farinella, A. (1998). "Finite element analysis of hyperelastic components." *Appl. Mech. Rev.*, 51, 303–320.

Ogden, R. W. (1972). "Large deformation isotropic elasticity: On the correlation of theory and experiment for compressible rubberlike solids." *Proc. R. Soc. London, Ser. A*, 328, 567–583.

Payne, A. R., and Whittaker, R. E. (1971). "Low strain dynamic properties of filled rubbers." *Rubber Chem. Technol.*, 44, 440–478.

Peng, S. H., and Chang, S. H. (1997). "A compressible approach in finite element analysis of rubber elastic materials." *Comput. Struct.*, 62, 573–593.

Peng, T. J., and Landel, R. F. (1972). "Stored energy function of rubber-like materials derived from simple tensile data." *J. Appl. Phys.*, 43, 3064–3067.

Quigley, C. J., Mead, J., and Johnson, A. R. (1995). "Large strain viscoelastic constitutive models for rubber. II: Determination of material constants." *Rubber Chem. Technol.*, 68, 230–247.

Ramberger, G. (2002). "Structural bearings and expansion joints for bridges." *Structural Engineering Documents 6*, International Association for Bridge and Structural Engineering, Zurich, Switzerland.

Rivlin, R. S. (1948a). "Large elastic deformations of isotropic materials: Fundamental concepts." *Philos. Trans. R. Soc. London, Ser. A*, 240, 459–490.

Rivlin, R. S. (1948b). "Large elastic deformations of isotropic materials IV. Further developments of the general theory." *Philos. Trans. R. Soc. London, Ser. A*, 241, 379–397.

Roeder, C. W., and Stanton, J. F. (1983). "Elastomeric bearings: State-of-the-art." *J. Struct. Eng.*, 109(12), 2853–2871.

Seibert, D. J., and Schöche, N. (2000). "Direct comparison of some recent rubber elasticity models." *Rubber Chem. Technol.*, 73, 366–384.

Simo, J. C., and Taylor, R. L. (1982). "Penalty function formulations for incompressible nonlinear elastics." *Comput. Methods Appl. Mech. Eng.*, 35, 107–118.

Taylor, R. L. (2000). *FEAP—A finite element analysis program, user manual, Version 7.3*, <http://www.ce.berkeley.edu/~rlt/feap/>, UC Berkeley.

Treloar, L. R. G. (1944). "Stress–strain data for vulcanized rubber under various types of deformations." *Trans. Faraday Soc.*, 29, 59–70.

Treloar, L. R. G. (1975). *The physics of rubber elasticity*, Clarendon, Oxford, U.K.

Tschoegl, N. W. (1972). "Constitutive equations for elastomers." *Rubber Chem. Technol.*, 45, 60–70.

Valanis, K. C., and Landel, R. F. (1967). "The strain-energy density function of a hyperelastic material in terms of the extension ratios." *J. Appl. Phys.*, 38, 2997–3002.

van den Bogert, P. A. J., and de Borst, R. (1994). "On the behavior of rubber-like materials in compression and shear." *Arch. Appl. Mech.*, 64, 136–146.

Ward, I. M. (1985). *Mechanical properties of solid polymers*, Wiley, New York.

Wiraguna, S. I. (2003). "Mechanical behavior of high damping rubber under shear deformation." MSc thesis, Saitama Univ., Saitama, Japan.

Wolfram, S. (1999). (1999). *The Mathematica Book*, 4th ed., Wolfram Media/Cambridge Univ. Press.

Yamashita, Y., and Kawabata, S. (1992). "Approximated form of the strain energy density function of carbon-black filled rubbers for industrial applications." *J. Soc. Rubber Ind. (Jpn.)*, 65, 517–528 (in Japanese).

Yeoh, O. H. (1990). "Characterization of elastic properties of carbon-black filled rubber vulcanizates." *Rubber Chem. Technol.*, 63, 792–805.

Yeoh, O. H. (1993). "Some forms of strain energy function for rubber." *Rubber Chem. Technol.*, 66, 754–771.

Yeoh, O. H. (1997). "On the Ogden stain-energy function." *Rubber Chem. Technol.*, 70, 175–182.

Yoshida, J., Abe, M., and Fujino, Y. (2004a). "Constitutive model of high-damping rubber materials." *J. Eng. Mech.*, 130(2), 129–141.

Yoshida, J., Abe, M., and Fujino, Y., and Watanabe, H. (2004b). "Three-dimensional finite-element analysis of high damping rubber bearings." *J. Eng. Mech.*, 130(5), 607–620.

Zienkiewicz, O. C., and Taylor, R. L. (1996). *The finite element method*, 4th Ed., McGraw-Hill, New York.